STATUS OF BEAM COMMISSIONING IN FRIB DRIVER LINAC*

T. Maruta[†], S. Cogan, K. Fukushima, M. Ikegami, S.H. Kim, S.M. Lidia, G. Machicoane, F. Marti,
D. Morris, P. Ostroumov, A. Plastun, J.T. Popielarski, J. Wei, T. Xu, T. Yoshimoto, T. Zhang,
Q. Zhao, S. Zhao

Facility for Rare Isotope Beams, Michigan State University, East Lansing, MI, USA

Abstract

The staged beam commissioning is underway in the Facility for Rare Isotope Beams (FRIB) being constructed at Michigan State University (MSU). The beam commissioning of the first linac segment (LS1) and a section of the first folding segment (FS1) took place in March 2019. Four different ion species were accelerated up to 20.3 MeV/u and transported to the beam dumps in FS1 with 100% transmission. This paper reports the beam measurement results performed during the commissioning of the LS1 and FS1.

INTRODUCTION

The FRIB is based on a continuous wave (CW) superconducting (SC) linear accelerator which is designed to deliver 400 kW heavy ion beams to the fragmentation target. The multi-stage beam commissioning activities started in the summer 2017 with expected completion in 2021 [1]. The direct current (DC) beam extracted from the electron cyclotron resonance ion source (ECRIS) is transported to the Radio Frequency Quadrupole (RFQ) located in the tunnel. Beam is bunched longitudinally by a multi-harmonic buncher (MHB) and then accelerated to 0.5 MeV/u in the RFQ followed by three SC linac segments (LS1 to LS3) to deliver beams to the fragmentation target. Two folding segments (FS1 and FS2) are connecting the linac segments and the beam will be transported to the production target by the beam delivery system (BDS). To reach the design beam energies of 200 MeV/u, the linac requires a charge stripper which is located at the end of LS1.

The beam commissioning of the LS1, shown in Fig.1, took place in the spring 2019 [2, 3]. Four ion species of ^{20}Ne, ^{40}Ar, ^{86}Kr and ^{129}Xe were accelerated to 20.3 MeV/u. The charge state distribution of each ion specie was measured after the 45° bending magnet.

The LS1 includes three CA type cryomodules housing four $\beta_{OPT} = 0.041$ SC quarter wave resonators (QWRs) and two 25-cm-long SC solenoids, and eleven CB type cryomodules containing eight $\beta_{OPT} = 0.085$ SC QWRs and three 50-cm-long SC solenoids, respectively. Their operating frequency is 80.5 MHz and design accelerating voltages are 0.81 and 1.78 MV. While a liquid lithium stripper is a main option for the high power operation, a carbon foil stripper was used for our measurements. The carbon foils of thicknesses of 0.4, 0.6 and 0.8 mg/cm^2, were mounted

on a stripper wheel. A charge selection slits are located after the 45° bending magnet of the FS1 to intercept unwanted charge states of the beam. The location of two beam dumps, FS1a and FS1b is shown in Fig.1. In addition to these dumps, a movable niobium plate after the third cryomodule was also used as a beam dump for beam studies in the upstream section, because the transportation of low energy beam to the beam dump FS1a requires too much tuning time.

A large variety of beam diagnostics devices was available during the beam commissioning in LS1 and FS1 including AC-coupled Beam Current Monitors (BCMs), Beam Position and Phase Monitors (BPMs), Halo Monitor Rings (HMRs), Profile Monitors (PMs), scintillator-based neutron monitors and parallel plate ion chambers.

An electrostatic chopper located in the LEBT was used to produce a pulsed beam structure necessary for BCM beam current measurements and control the average beam power.

BEAM COMMISSIONING

The stage three of the FRIB beam commissioning took place in the spring 2019 over the 3-week period. Only major beam commissioning procedures and beam parameters' measurements are discussed in this paper. More extended discussion of the beam commissioning results was presented in recent publication [3]. Both transverse and longitudinal tuning of the linac were performed with ^{40}Ar^{9+} beam. Then, all electromagnetic fields were scaled for other ion species according to the charge-to-mass ratio.

Longitudinal Tuning

At the beginning of the beam commissioning, the phases and amplitudes of each resonator were tuned by 360° phase scan and time-of-flight measurements using BPMs. The latter was applied to tune each MEBT buncher and each SC cavity. This procedure was applied at ~1 MV/m accelerating gradient to avoid transverse steering of the beam which strongly depends on the RF field phase. The cavity accelerating phase was set to the design value, which is typically equal to -30° from the maximum acceleration phase. The cavity accelerating gradient was calibrated by measuring the absolute beam energy. For robust TOF measurements by three BPM pairs were utilized. The BPM signal amplifiers have very high sensitivity, therefore stable measured data can be obtained for ~40 nA beam current. The accuracy of the absolute beam energy measurements is high, typically ~20 keV/u at 20.3 MeV/u. In this manner, the beam energy is known with high accuracy upstream of the SC cavity which is being set. In addition, the beam energy
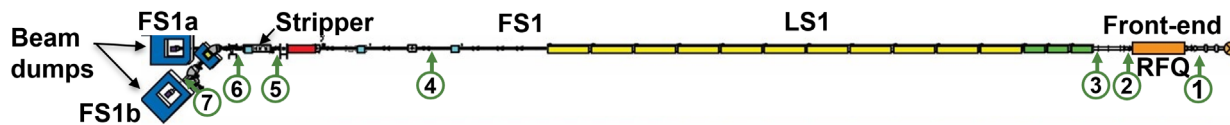
Figure 1: The beam line commissioned in the 3rd stage. The green and yellow boxes are CA type and CB type cryomodules. Stripper locates almost end of the straight section. The numbers show the location of BCMs to check the beam transmission along the beamline.

was measured after each $\beta_{OPT} = 0.041$ SC cavity with the silicon detector [2, 4].

During the phase scan procedure of the MEBT bunchers and the resonators in the CA, the beam was dumped in the retractable niobium plate installed in the warm box after the first three cryomodules to avoid uncontrolled beam spill in the following cryomodules due to the transverse mismatch at different beam energies. Argon beam was accelerated in the CAs to 1.5 MeV/u. The beam can be transported to the beam dump FS1a at any energy above 1.5 MeV/u by appropriate setting of the focusing solenoids and quadrupoles. The argon beam was accelerated to 20.3 MeV/u after completion of all resonators' setting. The beam energy was verified by both time-of-flight measurements and the first 45° bending magnet in FS1.

Transverse Matching

After completion of the resonators' tuning, the matching of transverse beam Twiss parameters was performed in the MEBT to minimize beam envelopes in the LS1 and avoid any detectable beam losses. Since there is only one profile monitor (PM) in the MEBT, the Twiss parameters were determined using a quadrupole scan procedure. In this procedure, the root mean square (RMS) beam sizes were measured while the quadrupole strength located upstream of the PM was varied. Figure 2 shows the RMS envelope (top) and normalized emittance (middle) of 133 eµA $^{40}Ar^{9+}$ beam along the MEBT and CA cryomodules. The reconstructed RMS emittance is close to the design emittance of 0.1 π mm-mrad as listed in Table 1. The beam matching to the SC section of the LS1 was performed using four MEBT quadrupoles. The maximum rms envelope size in the SC section was reduced by 5 mm. The optimized envelopes are shown by dotted lines in Fig. 2. No beam losses were observed in LS1. Since the solenoids couple the xx', yy' phase spaces, the 2D projected emittances vary along the LS1.

After completion of the MEBT matching, the transverse emittance in FS1 was measured by quadrupole scan. To avoid beam losses during the scan, four quadrupoles downstream of the PM were also adjusted for the Twiss parameters recovery [6]. Some emittance growth was observed in the LS1 as shown in Table 1.

Table 1: Transverse Normalized RMS Emittance in MEBT and FS1 of 133 eµA 40Ar Beam. The Emittance in Both Sections Were Obtained by Quadrupole Scans

Location	Horizontal	Vertical
MEBT [π mm-mrad]	0.13	0.11
FS1 [π mm-mrad]	0.12	0.13

Charge Stripping

The charge state distribution after the stripper was obtained by scanning the 45° bending magnet field with measuring the BPM signal magnitude just after the charge selector with a narrow gap. Figure 3 shows the average and standard deviation of charge state distributions of four ion species. Equilibrium charge states calculated by Baron's formula [7] are also plotted. The stripping foil thickness was 0.8 mg/cm^2 foil. Whereas the light ion species are fully stripped, the charge states of medium to heavy ions are lower than their equilibrium charge states. Therefore, thicker foil should be used for stripping of ions heavier than argon. The standard deviation of charge state distributions is close to the Baron formula.

Figure 3: Average charge state of four ion species after the 0.8 mg/cm^2 (red) carbon foil and Baron's formula (blue). The bar shows the standard deviation of the charge state distribution.
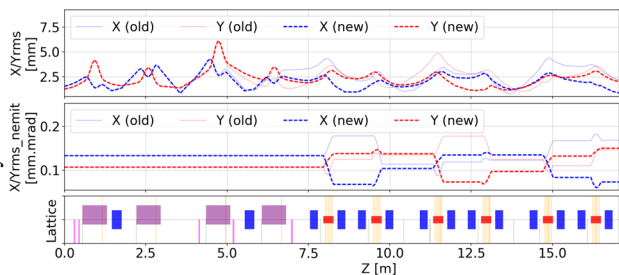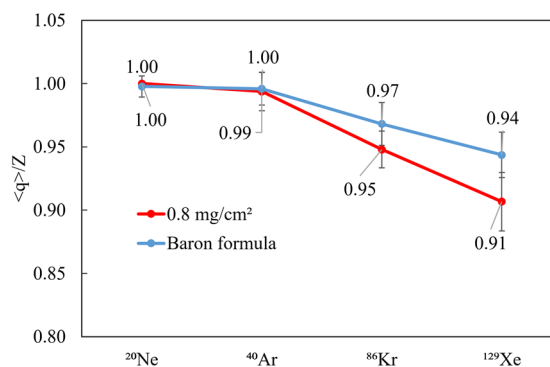

Figure 2: Beam envelope and emittance before and after MEBT transverse matching simulated by FLAME [5]. In the lattice plot, blue, red and purple boxes represent resonator, solenoid and quadrupole triplet, respectively.

The emittance growth in the stripping foil due to multiple scattering was measured for ^{20}Ne beam which is most suitable for these studies once it becomes fully stripping after the foil. The results are presented in Fig. 4. As can been seen, the measured data is consistent with the SRIM

[8] simulation. Based on these measurements, we recommend providing 1.5 mm rms beam size on the carbon foil for future beam commissioning as a compromise between the emittance growth and foil lifetime. Note, the beam size can be reduced to 0.5 mm when liquid lithium system is utilized as a charge stripper.
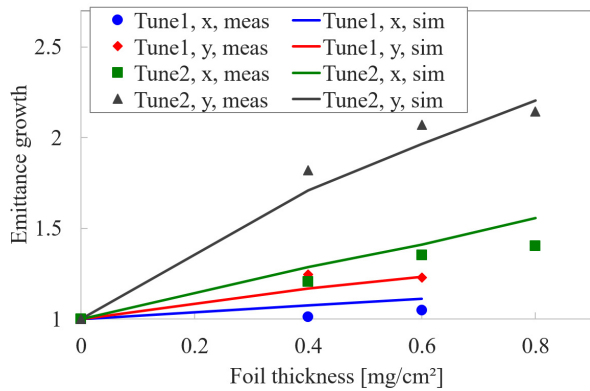

Figure 4: The rms emittance growth factor as a function of the foil thickness. Tune 1 corresponds to x_{rms} 1.4 mm and y_{rms} 1.5 mm. Tune 2 corresponds to x_{rms} 2.7 mm and y_{rms} 4.3 mm. The solid lines show calculated growth by SRIM simulation.

Increased Beam Power Tests

The tuning and setting of electromagnetic fields in all accelerator devices were performed with very low beam power, typically below 2 W. The beam power in LS1 was limited by the beam dump. The acceleration of high power equivalent beam was demonstrated in two regimes: (i) high peak current, low duty factor and (ii) low current CW beams. Figure 5 shows the BCMs readings at a high power equivalent beam acceleration with high peak current. The peak beam current was133 eμA corresponding to 30% of the FRIB design intensity. 0.8 mg/cm^2 carbon foil was inserted on the beamline. The FC in MEBT was opened at 21:27:05. The numbering corresponds to the BCMs locations of which are shown in Fig. 1. The beam transmission from the MEBT to FS1 is 100%. After the stripping of ^{40}Ar to charge states 17+ and 18+, the beam current doubles. The charge state 18+ is selected by the charge selector and then transported to FS1b.

SUMMARY

The first straight segment of the FRIB linac was successfully commissioned with four ion species. All beams were accelerated to 20.3 MeV/u without any notable beam losses. No transverse emittance growth in LS1 was observed after beam matching in the MEBT. The scaling of electromagnetic fields to different ion species worked well. Charge state distribution after the 0.8 mg/cm2 carbon stripper foil indicates that the thicker foil is necessary for medium to heavy ions to reach equilibrium charge state.
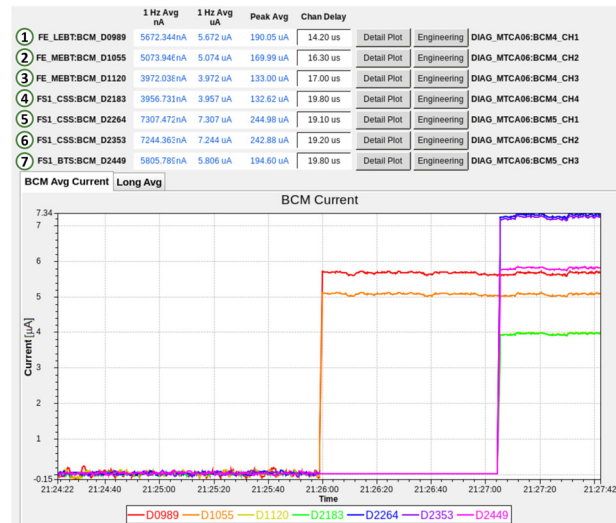

Figure 5: BCM readings during a high power test with a 0.8 mg/cm^2 foil. The location of BCMs are shown in Fig. 1.

All accelerator hardware showed very reliable operation within the design parameters space. Currently, installation of 12 cryomodules of $\beta_{OPT} = 0.29$ cavities and 12 cryomodules of $\beta_{OPT} = 0.53$ at Linac Segment 2 (LS2) is in progress. The commissioning of LS2 will take place in March-June 2020 with the goal to accelerate argon beam above 200 MeV/u.

REFERENCES

[1] J. Wei *et al.*, International Journal of Modern Physics E 28, 193000 (2019).

[2] P.N. Ostroumov *et al.*, "Heavy ion beam acceleration in the first three cryomodules at the Facility for Rare Isotope Beams at Michigan State University", *Phys. Rev. Accel. Beams,* vol. 22, p. 040101 (2019).

[3] P.N. Ostroumov *et al.*, "Beam commissioning in the first superconducting segment of the Facility for Rare Isotope Beams. Accepted for publication in Physical Review Accelerators and Beams", *Phys. Rev. Accel. Beams*, vol. 22, p. 080101 (2019).

[4] T. Maruta, P. N. Ostroumov, and Q. Zhao, "Longitudinal Beam Profile Measurement by Silicon Detector in Facility for Rare Isotope Beams at Michigan State University", presented at the NAPAC'19, Lansing, MI, USA, Sep. 2019, paper WEPLH01, this conference.

[5] Z. He, Y. Zhang, J. Wei, Z. Liu, and R.M. Talman, "Linear Envelope Model for Multicharge State Linac", *Phys. Rev. ST Accel. Beams*, vol. 17, p. 034001 (2014).

[6] K. Fukushima, T. Maruta, P. N. Ostroumov, and T. Yoshimoto, "No Beam-Loss Quadrupole Scan for Transverse Phase Space Measurements", presented at the NAPAC'19, Lansing, MI, USA, Sep. 2019, paper WEZBA3, this conference.

[7] E. Baron, M. Bajard, and Ch. Ricaud, "Charge exchange of very heavy ions in carbon foils and in the residual gas of GANIL cyclotrons", *Nucl. Instrum. Methods Phys. Res.*, Sect. A328, 177 (1993).

[8] The Stopping and Range of Ions in Matter, http://www.srim.org